Fermi National Accelerator Laboratory

FERMILAB-Pub-81/13-THY
January, 1981

Further Evidence for Flavor-Independence of the Quark-Antiquark Potential

C. QUIGG
Fermi National Accelerator Laboratory
P.O. Box 500, Batavia, Illinois 60510

and

JONATHAN L. ROSNER
School of Physics and Astronomy
University of Minnesota, Minneapolis, Minnesota 55455

(Received

ABSTRACT

An inverse-scattering algorithm is used to construct the interquark potential from the masses and leptonic widths of vector mesons. There is substantial agreement between potentials constructed from the 1S and 2S levels of the ψ family, and those based upon the 1S-4S levels of the T family. This agreement provides evidence that the quark-antiquark interaction is independent of heavy-quark flavor for interquark separations between about 0.1 and 1 fm. Self-consistency of the various determinations is explored at some length, and the uncertainties inherent in the method are investigated in detail. Predictions are made for electric-dipole transition rates in the T family, and the significance of future measurements for refining and extending present knowledge of the potential is discussed.

PACS Category Numbers: 12.40.Qq, 14.40.Pe

I. INTRODUCTION

The properties of bound states of heavy quarks and antiquarks reflect the character of the interquark interaction. It has been established that many features of the ψ and T resonances may be understood in the context of nonrelativistic quantum mechanics with a static central potential.[1] For the purpose of describing these quarkonium systems, the problem of determining the interaction between quarks thus may be framed as that of determining the interquark potential. Since the discovery of the charmonium (ψ) family in 1974,[2] much effort has been devoted to this task.

Exploration of the interquark potential has taken many forms. The asymptotic freedom of quantum chromodynamics suggests that at very short distances the potential is Coulomb-like.[3] At distances exceeding 1 fm, the relativistic string picture makes plausible a linear form for the potential.[4] Numerous interpolations, with varying degrees of theoretical motivation, have been advanced for the intermediate regime in which all the known levels lie.[5] Other work has been directed toward establishing the form of the interaction in the region of space occupied by the quarkonium levels, without particular regard to what may happen at much shorter or much longer distances. These methods, which rely on scaling properties of power-law potentials[6] or on the application of inverse-scattering

techniques, have the advantage of being free from theoretical biases about short- and long-distance behavior. They are correspondingly unable to test such biases effectively.

In this paper, we continue the program[7] of using inverse-scattering methods to construct the interquark potential from experimental information on the masses and leptonic widths of $^3S_1$ quarkonium levels. In the charmonium family there are two such levels, $\psi(3097)$ and $\psi(3686)$, below the charm threshold. In the upsilon threshold there are three $^3S_1$ states below flavor threshold [T(9434), T(9994), and T(10324)] and one, T(10545), just above threshold. In a previous publication,[8] a "best" potential constructed from the two ψ-states was compared with a potential implied by the 1S and 2S T levels, the only ones for which detailed information was then available. In the spatial region where such a comparison makes sense, the close agreement between the two potentials may be taken as evidence that the force between quarks is independent of flavor.

Experimental study of the higher T levels[9] now makes it possible to extend the comparison to larger interquark separations, and to make more decisive tests of the hypothesis of flavor-independence.[10] On this basis we find that the ψ and T potentials agree well in the interval $0.1\ \text{fm} \lesssim r \lesssim 1\ \text{fm}$. Quantitative measures of the similarity are found by using the potential constructed from ψ-data to

compute T-observables, and vice versa.

The inverse scattering method relies upon experimental information about the quarkonium levels and about quarkonium wavefunctions at the origin. The latter are deduced from measured leptonic decay widths, but the precise connection between the two is uncertain. We therefore vary the constant of proportionality between the square of the wavefunction and the leptonic width, to study the effect upon our results and conclusions. It is found that the major effect of this variation is confined to short distances ($r<0.1$ fm), so that charmonium and upsilon data have little to say about this coefficient of proportionality. Other methods are also subject to this ambiguity, but less directly.

Using the potentials constructed from the $^3S_1$ quarkonium levels, we may make a number of predictions which will serve to test and refine our knowledge of the strong interaction. Under the assumption that odd- and even-angular momentum levels are determined by a common interaction (which is to say that exchange forces are absent), it is straightforward to compute the positions of orbital excitations and to estimate electric dipole transition rates between levels. In common with other authors,[5,11] we arrive at predicted transition rates which seem too large, compared with measured rates in charmonium, by a factor of two to four. The predictions for the upsilon

family are yet to be tested, but seem to indicate that electromagnetic transitions are more readily observable than simple scaling arguments[12] would suggest.

The inverse-scattering method provides a representation of the potential in the region of importance for existing data. No less significantly, it helps to define the regions in space in which, on the basis of quarkonium information, we are ignorant of the interquark interaction. This information in turn helps us to judge the potential value of a variety of measurements which may be carried out in the future, and to sharpen questions to be asked of experiment.

The body of this article is organized as follows. In Section II we give a very brief review of the inverse scattering algorithm and apply it to the construction of ψ and T potentials. Ambiguities (principally arising from uncertainties in the connection between leptonic widths and wavefunction normalization) in the determination of the potentials are investigated, and the consistency of the various potentials is judged. Calculations of the E1 transition rates and a discussion of their implications occupy Section III. In the concluding Section IV we discuss the extent to which the interquark potential is known and where the uncertainties lie, and assess the importance of additional experimental information.

II. CONSTRUCTION OF POTENTIALS

A. Review of the Method

The familiar "direct" problem of the quantum mechanics of nonrelativistic bound states consists of solving for the eigenvalues and eigenfunctions of the Schrödinger equation

$$\left[-\frac{\nabla^2}{2\mu} + V(r)\right] \Psi(\underset{\sim}{r}) = E\Psi(\underset{\sim}{r}) \quad , \tag{1}$$

for a specified central potential $V(r)$ and reduced mass μ. The inverse-scattering (or, more aptly, inverse-bound-state) method,[13,7] which we shall employ, is a technique for constructing the potential from information about the S-matrix.

For orientation, let us consider the problem of determining a one-dimensional potential $V(x)$ which approaches a constant at infinity,

$$V(\pm\infty) \to E_0, \tag{2}$$

and supports N bound states of a system with reduced mass μ. Limited information about the bound states does not, in general, suffice to specify the potential. For example, many different potentials yield the same spectrum of bound-state energy levels. In the most general circumstances, two pieces of information about each bound

state (e.g. the energy level and a wavefunction normalization as $x \to +\infty$) and knowledge of the scattering phase shifts throughout the continuum are required to determine the potential. However, a specific class of potentials which are both symmetric,

$$V(x) = V(-x), \tag{3}$$

and reflectionless in the continuum are determined uniquely by the positions of their bound states.[14,7] The restriction to symmetric potentials means that only a single piece of information is required of each bound state. The absence of reflection for one-dimensional scattering eliminates the need for explicit phase-shift information, and reduces an integral equation for the potential to an albegraic equation.

If the bound state energies are $E_i (i=1,\ldots,N)$, then the symmetric, reflectionless potential which satisfies (2) is uniquely given by[16]

$$V(x) = E_0 - \frac{1}{\mu} \frac{d^2}{dx^2} \ln D(x), \tag{4}$$

with

$$D(x) = \sum_{S} \Pi(S,\bar{S}) \cosh\left[x\left(\sum_{m\in S} \kappa_m - \sum_{n\in\bar{S}} \kappa_n\right)\right], \tag{5}$$

and

$$\Pi(S,\bar{S}) = \prod_{\substack{m\in S \\ n\in\bar{S}}} \left|\frac{\kappa_m+\kappa_n}{\kappa_m-\kappa_n}\right| , \tag{6}$$

where

$$\kappa_i^2 = 2\mu(E_0-E_i). \tag{7}$$

In equations (5) and (6), S denotes a subset of the integers 1,...,N, and $\bar{S}$ is its complement. Algebraic expressions have also been given for the bound-state wavefunctions.

The foregoing results are exact, but limited to potentials with a finite discrete spectrum which satisfy the asymptotic condition (2). It has been proposed[15] that symmetric confining potentials, which possess only a discrete spectrum, can be systematically approximated within a limited region of space by symmetric reflectionless potentials. In practice, a symmetric reflectionless potential which binds the first N levels of a confining potential and approaches a value

$$V_N(\infty) = E_0(N) \equiv \frac{1}{2}(E_N+E_{N+1}), \tag{8}$$

is found to reproduce the confining potential within the classically-allowed region for the N levels. Specific illustrations for the linear, harmonic oscillator, and infinite square well potentials are presented in refs. 15 and 16.

The symmetry requirement (3) ensures that the one-dimensional problem will be the analog of the s-wave problem for a central potential in three dimensions. Corresponding to the three-dimensional s-wave solutions $\Psi_n(r)$ are the odd-parity solutions

$$\psi_{2n}(x) = -\psi_{2n}(-x), \tag{9}$$

in one dimension. With the usual normalization conditions,

$$\int d^3r \, |\Psi_n(r)|^2 = 1 \tag{10}$$

and

$$\int_{-\infty}^{\infty} dx \, |\psi_{2n}(x)|^2 = 1, \tag{11}$$

the relation between the three-dimensional s-wave solution and the one-dimensional solution is

$$(2\pi)^{1/2} \Psi_n(r) = \psi_{2n}(r)/r. \tag{12}$$

So far as the three-dimensional s-wave problem is concerned, the even-parity levels which lie at $E_1, E_3, \ldots$ are unphysical so that information about them is not directly accessible. However, in symmetric reflectionless potentials, the properties of even-parity and odd-parity solutions are intimately connected, especially when the number of even- and odd-parity levels is equal. Consider a symmetric, reflectionless potential which supports an even number N=2L of bound states, and define the function

$$f(E) \equiv \prod_{k=1}^{L} \left(\frac{E-E_{2k-1}}{E-E_{2k}} \right) \quad . \tag{13}$$

Then it may be shown[16] that in a symmetric reflectionless potential for which the continuum begins at E_0, as in eq. (2),

$$f(E) = 1 + 2 \sum_{k=1}^{L} \frac{|\psi'_{2k}(0)|^2}{(E_0-E_{2k})^{1/2}(E-E_{2k})} \quad . \tag{14}$$

Thus, if the positions of the odd-parity solutions and the slopes at the origin of the odd-parity wavefunctions are known, the function f(E) may be evaluated as the right-hand-side of eq.(14). The definition (13) shows that the zeroes of f(E) are none other than the positions of the "unphysical" levels, E_{2k-1}.

In the (N=2L)-level s-wave problem in three dimensions it is necessary to choose the continuum energy $E_0(2L)$ in accord with the condition (8), without knowing the position of the unphysical level E_{2L+1}. If E_{2L+2} is known, we interpolate:

$$E_0(2L) \approx \frac{3E_{2L}+E_{2L+2}}{4} \quad . \tag{15}$$

Otherwise, an extrapolation

$$E_0(2L) \approx \frac{5E_{2L}-E_{2L-2}}{4} \tag{16}$$

will yield a suitable estimate.

The slope of the odd-parity, one-dimensional wavefunction at the origin, which is required for the evaluation of f(E) by means of (14), is related by eq.(12) to the s-wave wavefunction at the origin as

$$|\psi'_{2n}(0)|^2 = 2\pi|\Psi_n(0)|^2 \quad . \tag{17}$$

For n^3S_1 bound states of heavy quarks and antiquarks ($Q\bar{Q}$), $|\Psi_n(0)|^2$ is related to the leptonic decay rate by [17]

$$|\Psi_n(0)|^2 = (3/16\pi N_c \alpha^2 e_Q^2)\cdot\rho\cdot M_n^2 \Gamma(V_n \to e^+e^-) \quad , \tag{18}$$

where N_c is the number of colors of the Q-quark and e_Q is its charge, $\alpha \approx 1/137$ is the fine-structure constant, and M_n is the mass of the vector state V_n. The multiplicative correction factor ρ is equal to unity in the nonrelativistic limit. In a purely Coulombic quarkonium system, quantum chromodynamics yields a correction

$$\rho = \left[1 - \frac{16\alpha_s}{3\pi} + \mathcal{O}(\beta^2)\right]^{-1} \quad , \tag{19}$$

where α_s is the strong-interaction coupling constant and β is the speed of the bound quark. Although the known quarkonium families are decidedly non-Coulombic, the belief that the strong coupling constant may be as large as $\alpha_s = 0.2\text{-}0.3$ for ψ and Υ has led many authors to suspect that ρ may be appreciably greater than one. A detailed argument for extending (19) beyond purely Coulombic systems has been given in ref. 11.

B. Applications to Quarkonium

Using the techniques recalled above, we construct potentials from the experimental observations summarized in Table I. Our choices of the parameter E_0 are guided by

eq.(15), for potentials deduced from charmonium, and eq.(16), for those based upon upsilon data. We take as representative values of the multiplicative correction to the Van Royen-Weisskopf formula (18) $\rho=1$ (which corresponds to no correction), and $\rho=1.4$ and 2. We believe, but cannot prove, that $\rho=2$ represents a larger correction than is plausible, and intend that the extremes $\rho=(1,2)$ bracket the true value. For the upsilon family, the parameter ρ can also be regarded as allowing for variations in the still uncertain absolute scale of leptonic widths.

In the case of charmonium, the potential constructed under the assumption that $\rho=1$ has been discussed extensively in earlier publications.[19,8] Although only s-wave information is used systematically in the inverse-scattering algorithm, information about other partial waves may be used to discriminate among potentials constructed under varying assumptions for E_0 and the quark mass. To employ p-wave data in this manner entails the assumption that exchange forces can safely be neglected. The value of the charmed quark mass which reproduces the observed center of gravity of the p-wave ψ levels, $\langle M(\chi)\rangle=3.52$ GeV/c^2, is rather low: $m_c=1.1$ GeV/c^2. For choices other than $\rho=1$, it is possible to adjust the quark mass to maintain agreement with experiment, as shown in Table II. Also shown in Table II are the properties of the T states implied by these charmonium potentials. In each case, the mass of the b-quark has been

chosen to give an T mass of 9.434 GeV/c^2. The three potentials are depicted in Fig.1(a)-(c). On the left-hand-side of each plot are shown the input 1^3S_1 and 2^3S_1 ψ levels (solid lines) and the calculated positions of the first p-waves,[20] the 2^3P_J levels (dashed lines). On the right-hand-side of each graph are plotted the $^3S_1$ T levels (solid lines) and the 2^3P_J (χ_b) states (dashed lines).

The three charmonium potentials are compared in Fig.2. In the range 0.5 $GeV^{-1} \lesssim r \lesssim 5$ GeV^{-1}, the potentials depend approximately logarithmically upon the interquark separation, as expected on the basis of scaling arguments.[6] The local fluctuations are artifacts of the reflectionless approximant technique. The small systematic difference between the three charmonium potentials is that the potentials corresponding to larger values of ρ and m_c are somewhat more spatially compact. This is reflected in the sizes of states, listed in Table II. Also shown in Fig.2 (as the dotted line) is the shape of the QCD-inspired potential of Buchmüller and Tye,[11] which is typical of explicit potentials that provide a good representation of ψ and T data. In the region of space to which charmonium observables are sensitive, it provides a smooth interpolation of the inverse scattering results.

The potential constructed from the T data collected in Table I under the assumption that ρ=1 has also been discussed before.[10] Only $^3S_1$ levels of the upsilon family

are known at present, so it is not yet possible to use the p-wave spectrum to select a best value of the b-quark mass for a particular choice of the parameter ρ. We find, as shown in Fig.3, that within reasonable bounds the value of m_b does not appreciably affect the shape of the potential. The potential constructed for $\rho=1$, $m_b=5$ GeV/c^2 (dashed line) is slightly shallower at very short distances than that constructed for $\rho=1$, $m_b=4.5$ GeV/c^2 (solid line). The p-wave ($b\bar{b}$) levels are only mildly sensitive to this difference:

$$M(T') - \langle M(\chi_b) \rangle = \begin{cases} 142 \text{ MeV}/c^2, \text{ for } m_b = 4.5 \text{ GeV}/c^2 \\ 148 \text{ MeV}/c^2, \text{ for } m_b = 5 \text{ GeV}/c^2 \end{cases} .$$

This lack of sensitivity persists for larger values of ρ, and we conclude that the exact choice of m_b is of little consequence.

To facilitate comparison with the charmonium potentials, we select values of m_b close to those shown in Table II. The results are given in Table III. As ρ increases, the ψ'-χ_b (2S-2P) spacing decreases. With a suitable choice of the charmed quark mass, properties of the charmonium system are reproduced satisfactorily. A slight increase in the assumed values of m_b would improve the agreement, but we see no need to engage in such fine-tuning.

The potentials based on parameters in Table III are shown in Fig.4(a)-(c). On the right-hand side of each graph are plotted the input 1^3S_1-4^3S_1 upsilon levels (solid lines) and the calculated center of gravity of the $2^3P_J(\chi_b)$ states (dashed lines). The calculated positions of the ψ, ψ', and χ_c levels are plotted on the left-hand side of each diagram.

The three upsilon potentials are compared in Fig. 5. They are essentially indistinguishable for interquark separations larger than 0.4 GeV^{-1} (0.08 fm). They also approximately coincide with other potentials that reproduce the data, such as the Buchmüller-Tye potential[11] which is shown by the dotted line. Like the charmonium potentials in Fig. 2, the upsilon potentials behave approximately logarithmically in the interval $0.5\ GeV^{-1} \lesssim r \lesssim 5\ GeV^{-1}$. At distances smaller than 0.4 GeV^{-1}, there is considerable variation among the potentials. This provides a gauge of our current ignorance of the interaction between quarks at short distances. In the companion to this article[21] we explore the degree to which the range of possibilities can be narrowed by observations of more massive quarkonium families.

The potentials constructed from the ψ and T families are compared with one another for equal values of the parameter ρ in Fig. 6, where they have been superposed by requiring that the $\psi(3097)$ levels coincide. The agreement in each case is excellent for $r \gtrsim 0.5\ GeV^{-1}$ (0.1 fm), where

both quarkonium systems provide information. The comparison provides direct evidence that the strong (quark-antiquark) interaction is flavor-independent in the range 0.1 fm $\leq r \leq$ 1 fm. This conclusion is supported by the quantitative agreement of predictions from ψ-potentials with T-observables shown in Table II and of predictions from T-potentials with ψ-observables shown in Table III.

III. ELECTRIC DIPOLE TRANSITIONS AND HIGHER ($b\bar{b}$) LEVELS

With quarkonium potentials and Schrödinger wavefunctions in our possession, we may elaborate other consequences of the nonrelativistic description. Assuming that the $^3S_1$ potentials constructed using inverse scattering techniques give, when supplemented by the appropriate centrifugal potential, reliable descriptions of the orbital excitations, it is a simple matter to compute the quarkonium spectrum in detail. The positions of the 2^3P_J levels of charmonium, computed in the this manner, provided a nontrivial test of the potentials. The results of an analogous calculation for the excited T states, using the T potentials, are summarized in Table IV and Fig. 7. Predictions for these excited states are rather insensitive to the variations explored in Table III. Also given in Table IV and Fig. 7 are the predictions of a representative

explicit potential[11] which are, for the most part, similar to those of the inverse-scattering technique. We shall have more to say about this comparison below.

Further tests of the nonrelativistic description are made possible by the experimental study of electric dipole transition rates, which are sensitive to the spatial structure of the wavefunctions. For the S → P transitions of interest, the transition rates are given by

$$\left.\begin{matrix}\Gamma(n^3S_1 \to n'^3P_J + \gamma) \\ \text{or} \\ \Gamma(n^3P_J \to n'^3S_1 + \gamma)\end{matrix}\right\} = \frac{4\alpha^2 e_Q^2 k_\gamma^3}{27}(2J_f+1)|\langle f|r|i\rangle|^2 \quad , \quad (20)$$

where e_Q is the quark charge, k_γ is the photon momentum, and J_f is the spin of the final quarkonium state. The matrix element of the coordinate between initial and final states can be evaluated given any set of wavefunctions, and in particular those implied by the potentials constructed in Section IIB.

The masses[18] of the $2^3P_J(\chi_J)$ levels of charmonium have been determined from the observation of electromagnetic transitions. For this family, the fine-structure splittings are therefore known (although not entirely understood[22]), and it is possible to estimate E1 transition rates involving the individual p-wave states with masses

3551 MeV/c^2, $\chi_2(J^{PC}=2^{++})$;

3507 MeV/c^2, $\chi_1(J^{PC}=1^{++})$;

3414 MeV/c^2, $\chi_0(J^{PC}=0^{++})$.

The matrix elements and transition rates computed using the potentials characterized in Table II and Table III are presented in Table V. As noted before, larger values of the parameter ρ (which are correlated with larger quark masses) correspond to systems which are more spatially compact. The dipole matrix elements are therefore smaller, and so are the predicted transition rates. The predicted rates for the 2S-2P transitions are nevertheless far above the measured values of 16±5 keV, even for the case $\rho=2$, $m_c=1.7$ GeV/c^2. This failure, by factors of two or three, is common to most potential models and is not appreciably improved by the inclusion of coupled-channel effects.[23]

The uncertain position of the 2^3P_J levels in the Υ family introduces an additional variation in the predicted $\Upsilon' \to \chi_b + \gamma$ and $\chi_b \to \Upsilon + \gamma$ transition rates. These are computed in Table VI, neglecting fine-structure effects. The ψ and Υ potentials lead to quite similar matrix elements, but the transition rates differ appreciably. Most of this difference derives from the variation in χ_b positions as reflected in the k_γ^3 factor in eq.(20). The predictions for the 2S-2P transition rates are expected to be particularly sensitive to fine structure. One estimate of these effects

is given in ref. 12.

If relativistic effects should be responsible for the discrepancy between predicted and observed E1 transition rates in charmonium, it would be reasonable to expect that the predictions of Table VI would be more reliable for the T family. This would bode well for observation of the 2S-2P transitions. As an example, from Table VI we expect $\Gamma(T' \to \chi_1 + \gamma)$ to range between 0.8 and 1.2 keV if the 2S-2P splitting is approximately 100 MeV, as given by the ψ-potentials, or between 1.6 and 2.6 keV if the 2S-2P splitting is close to 130 MeV, as given by the T-potentials. (The $J^{PC}=1^{++}$ state is expected to be least displaced from the 2^3P_J center of gravity.) Even if the total width of T' is as large as 50 keV,[24] a 5% branching ratio for the $T' \to \chi_1 + \gamma$ transition is entirely within prospect. This estimate is much more favorable for observation than the value of 1% deduced[12] by scaling from charmonium.

Because the predicted positions of the higher $(b\bar{b})$ levels are similar in the three potentials constructed from upsilon observables, we expect that photon energies for transitions involving these levels can be estimated fairly reliably. The rather narrow range of predicted E1 transition rates (neglecting fine structure) is exhibited in Table VII, where predictions of the extreme $\rho=1$ and 2 potentials are tabulated. Of special inerest is the expectation that the 3S-3P transition rate,

$$\Gamma(T(10.32) \to \chi_J(10.22) + \gamma) \approx (2J+1) \times 1 \text{ keV} \quad , \qquad (21)$$

should exceed the corresponding 2S-2P transition rate,

$$\Gamma(T(9.99) \to \chi_J(9.86) + \gamma) \approx (2J+1) \times 0.7 \text{ keV} \quad . \qquad (22)$$

This is a consequence of the fact that the dipole matrix element is larger for the 3S-3P transition than for the 2S-2P transition, which in turn reflects the larger size of the n=3 states.[25]

An intriguing possibility exists for placing rather tight bounds on the b-flavor threshold, given by twice the B-meson ($b\bar{q}$) mass. There is considerable evidence that T(4S, 10.545) lies above flavor threshold. The narrowness of T(3S, 10.324), many explicit calculations,[26] and general theorems[27] all suggest that $2M_B \geq M(T(3S))$. However, if the hadronic production of T(3S) proceeds by a cascade from the 4P-level, the indications for T(3S) in pp collisions[24] would require the 4P also to lie below flavor threshold. Thus we would have

$$M(T(4S)) \geq 2M_B \geq M(T(4P)) \quad , \qquad (23)$$

or

$$5.272 \text{ GeV}/c^2 \geq M_B \geq 5.23 \text{ GeV}/c^2 \quad .[28] \qquad (24)$$

The estimate[26,27]

$$M_B \approx M_D + (m_b - m_c) \tag{25}$$

then leads to the conclusion that the quark mass difference is

$$(m_b - m_c) \approx 3.38 \pm 0.03 \text{ GeV}/c^2 \quad . \tag{26}$$

This difference is lowered by at most 1% if reduced mass and hyperfine effects are taken into account as suggested in ref. 27. The quark masses in Table II and III satisfy (26) for ρ=1.4 and 2. For ρ=1, the quark mass difference is just slightly too large. Literally applied, these arguments would imply that in the case ρ=1 the 4S level should lie just below flavor threshold.

IV. OUTLOOK

We have shown that charmonium and upsilon data determine the interquark potential at distances between 0.1 fm and 1 fm, without recourse to theoretical prejudices for the form of the potential at very large or very short distances. What are the prospects for extending the range over which the form of the interaction is known?

At distances exceeding 1 fm, corresponding to states above flavor threshold, there is as yet little support for the popular linear potential from the $(c\bar{c})$ and $(b\bar{b})$ systems.

The inverse scattering method does not now address this issue, because it is restricted to distances smaller than the classical turning point of the highest level included in the determination of the potential. This situation is unlikely to improve significantly, because the inclusion of higher excited states extending well above flavor threshold would be a questionable procedure. Above the threshold, a single-channel analysis is surely inadequate, and the meaning of a static potential becomes obscure for short-lived states. What can be said is that the expected linear behavior does not appear to set in at such small distances as suggested in the potential of Buchmüller and Tye[11] (dotted line in Figs. 2 and 5). This judgment is based upon the position of the $\Upsilon(4S)$ level shown in Fig. 7, which lies some 50 MeV/c^2 below the prediction of ref. 11. To invoke shifts associated with coupled-channel effects[23] to dispose of this discrepancy seems to us to undercut the notion of a static potential. The utility of the higher-lying charmonium states $\psi(4.03)$, $\psi(4.16)$, and $\psi(4.41)$ is limited by the uncertainty of their spectroscopic assignments and by the difficulty of measuring their leptonic widths. The positions and leptonic widths of the $\Upsilon(\geq 5S)$ levels may be a superior probe of the onset of linear behavior.

At distances between about 0.01 and 0.1 fm, our ignorance of the quark-antiquark interaction may be assayed from Fig. 5. The position of the $T(2^3P_J)$ center-of-gravity can help to discriminate among the possibilities, because the 2S-2P splitting is predicted to be different in the three T-potentials shown:

$$M(T') - \langle M(\chi_b)\rangle = \begin{cases} 142\ \text{MeV}/c^2, & \rho=1 \ ; \\ 132\ \text{MeV}/c^2, & \rho=1.4 \ ; \\ 121\ \text{MeV}/c^2, & \rho=2 \ . \end{cases} \qquad (27)$$

Better determinations of the ψ and T leptonic widths can also sharpen our knowledge of the interaction. However, the decisive information on quark-antiquark interactions at shorter distances must be supplied by new, heavier quarks. It is known from electron-positron annihilations[29] that if another charge-2/3 quark ("t-quark") exists, its mass must exceed about 18 GeV/c^2. It is conceivable, but unlikely, that another charge (-1/3) quark could have escaped detection at lower masses. In the following paper we explore the degree to which the next quarkonium family can provide new information on the force between quarks at short distances.

ACKNOWLEDGMENTS

Fermilab is operated by Universities Research Association, under contract with the United States Department of Energy. Work at the University of Minnesota was supported in part by the Department of Energy under Contract No. EY-76-C-02-1764. Part of this research was carried out during visits by J.L.R. to Cornell University and Fermilab. He wishes to thank K. Gottfried, D. Yennie, and C. Quigg for extending the generous hospitality of these institutions.

Discussions with K. Adams, O. Alvarez, J.D. Bjorken, W. Buchmüller, D. Creamer, E. Eichten, K. Gottfried, S. Herb, G.P. Lepage, P. Moxhay, M. Peskin, T.-M. Yan, and others at Cornell, Fermilab, and Minnesota are gratefully acknowledged. It is a pleasure to recognize the contributions of H.B. Thacker and J.F. Schonfeld to earlier phases of this program.

FOOTNOTES AND REFERENCES

1. J.D. Jackson, in Proc. 1977 European Conference on Particle Physics, Budapest, Hungary, edited by L. Jenik and I. Montvay (Central Research Institute for Physics, Budapest), Vol. I, p. 603; K. Gottfried, in Proc. 1977 International Symposium on Lepton and Photon Interactions at High Energies, Hamburg, edited by F. Gutbrod (DESY, Hamburg), p. 667; V.A. Novikov, L.B. Okun, M.A. Shifman, A.I. Vainshtein, M.B. Voloshin, and V.I. Zakharov, Phys. Rep. 41C, 1 (1978); T. Appelquist, R.M. Barnett, and K. Lane, Ann. Rev. Nucl. Part. Sci. 28, 387 (1978); E. Eichten, in New Results in High Energy Physics-1978 (Vanderbilt Conference), edited by R.S. Panvini and S.E. Csorna (AIP, New York), p. 252; J.D. Jackson, C. Quigg, and J.L. Rosner, in Proc. XIX International Conference on High Energy Physics, Tokyo, 1978, edited by S. Homma, M. Kawaguchi, and H. Miyazawa (Physical Society of Japan, Tokyo, 1979), p. 391; M. Krammer and H. Krasemann, "Quarkonium," in New Phenomena in Lepton-Hadron Physics (NATO Advanced Study Institutes Series: Series B, Physics; v.49), edited by D.E.C. Fries and J. Wess (Plenum, New York and London, 1979), p. 161; M. Krammer and H. Krasemann, "Quarkonia," in Quarks and Leptons as Fundamental Particles, ed. P. Urban, Acta Phys. Austriaca, Suppl. XXI, 259 (Springer-Verlag, Vienna and New York, 1979); C. Quigg, in Proceedings of the 1979 International Symposium on Lepton and Photon Interactions at High Energies, edited by T.B.W. Kirk and H.D.I. Abarbanel (Fermilab, Batavia, Illinois, 1980), p. 239; J.L. Rosner, in Particles and Fields - 1979, edited by B. Margolis

and D.G. Stairs (American Institute of Physics, New York, 1980), p. 325; C. Quigg and J.L. Rosner, Phys. Rep. 56C, 167 (1979); H. Grosse and A. Martin, Phys. Rep. 60C, 341 (1980); K. Gottfried, in High Energy e^+e^- Interactions (Vanderbilt, 1980), edited by R.S. Panvini and S.E. Csorna (American Institute of Physics, New York) p. 88; K. Berkelman, "New Flavor Spectroscopy," Cornell report CLNS 80/470 (unpublished); J.L. Rosner, "Quark Models," Lectures given at the NATO Advanced Study Institute, "Techniques and Concepts of High-Energy Physics," held at St. Croix, U.S. Virgin Islands, July 2-13, 1980 (to be published).

2. J.J. Aubert, et al., Phys. Rev. Lett. 33, 1404 (1974); J.E. Augustin, et al., ibid., 33, 1406 (1976); G.S. Abrams, et al., ibid., 33, 1453 (1974).

3. T. Appelquist and H.D. Politzer, Phys. Rev. Lett. 34, 43 (1975). The idea of asymptotic freedom is developed in D.J. Gross and F. Wilczek, Phys. Rev. Lett. 30, 1343 (1973); Phys. Rev. D8, 3633 (1973); ibid., D9, 980 (1974); H.D. Politzer, Phys. Rev. Lett. 30, 1346 (1973); Phys. Rep. 14C, 129 (1974).

4. Y. Nambu, Phys. Rev. D10, 4262 (1974).

5. E. Eichten, et al., Phys. Rev. Lett. 34, 369 (1975); ibid., 36, 500 (1976); Phys. Rev. D17, 3090 (1978); ibid., D21, 203 (1980); ibid., D21, 313E (1980); P. Ditsas, N.A. McDougall, and R.G. Moorhouse, Nucl. Phys. B146, 191 (1978); B. Margolis, R. Roskies, and N. De Takacsy, contribution to the IVth European Antiproton Conference, Barr, France (1978, unpublished); G. Bhanot and S. Rudaz, Phys. Lett. 78B, 119 (1978); W. Celmaster, H. Georgi, and M. Machacek, Phys. Rev. D17, 879 (1978); W. Celmaster and

F. Henyey, Phys. Rev. D18, 1688 (1978); R. Carlitz and D. Creamer, Ann. Phys. (N.Y.) 118, 429 (1979); R. Levine and Y. Tomozawa, Phys. Rev. D19, 1572 (1979), D21, 840 (1980); J.L. Richardson, Phys. Lett. 82B, 272 (1979); H. Krasemann and S. Ono, Nucl. Phys. B154, 283 (1979); G. Fogleman, D.B. Lichtenberg, and J.G. Wills, Nuovo Cim. Lett. 26, 369 (1979); W. Buchmüller, G. Grunberg, and S.-H. H. Tye, Phys. Rev. Lett. 45, 103 (1980); 45, 587E (1980).

6. C. Quigg and J.L. Rosner, Phys. Lett. 71B, 153 (1977); Comments Nucl. Part. Phys. 8, 11 (1978); M. Machacek and Y. Tomozawa, Ann. Phys. (N.Y.) 110, 407 (1978); C. Quigg, ref. 1; J.L. Rosner, ref. 1; C. Quigg and J.L. Rosner, ref. 1; A. Martin, Phys. Lett. 93B, 338 (1980); CERN report No. TH.2980 (1980, unpublished).

7. H.B. Thacker, C. Quigg, and J.L. Rosner, Phys. Rev. D18, 274 (1978); D18, 287 (1978); H. Grosse and A. Martin, Nucl. Phys. B148, 413 (1979); J.F. Schonfeld, et al., Ann. Phys. (N.Y.) 128, 1 (1980). I. Sabba Stefanescu, Karlsruhe report no. TKP 80-20 (unpublished).

8. C. Quigg, H.B. Thacker, and J.L. Rosner, Phys. Rev. D21, 234 (1980).

9. S.W. Herb, et al., Phys. Rev. Lett. 39, 252 (1977); W.R. Innes, et al., ibid., 39, 1240 (1977); ibid., 39, 1640E (1977); K. Ueno, et al., ibid., 42, 486 (1979); Ch. Berger, et al., Phys. Lett. 76B, 243 (1978); Z. Phys. C1, 343 (1979); C.W. Darden, et al., Phys. Lett. 76B, 246 (1978); ibid., 80B, 419 (1979); J. Bienlein, et al., ibid., 78B, 360 (1978); D. Andrews, et al., Phys. Rev. Lett. 44, 1108 (1980); ibid., 45, 219 (1980); T. Böhringer, et al., ibid., 44, 1111 (1980); ibid., 45, 222 (1980); G.C. Moneti, et al.,

Syracuse report no. HEPSY 15-80 (1980, unpublished); C. Bebek, et al., Phys. Rev. Lett. 46, 84 (1981); B. Niczyporuk, et al., ibid., 46, 92 (1981). An up-to-date summary is given by Berkelman, ref. 1.

10. C. Quigg and J.L. Rosner, Fermilab-Conf-80/75-THY (to appear in Proc. XXth International Conference on High Energy Physics, Madison, 1980).

11. W. Buchmüller and S.-H. H. Tye, Fermilab-80/94-THY (unpublished).

12. J.L. Rosner, "Quark Models," ref. 1.

13. I.M. Gel'fand and B.M. Levitan, Amer. Math. Soc. Trans. 1, 253 (1955); I. Kay and H.E. Moses, J. Appl. Phys. 27, 1503 (1956); C.S. Gardner, J.M. Greene, M.D. Kruskal, and R.M. Miura, Phys. Rev. Lett. 19, 1095 (1967); Comm. Pure Appl. Math. 27, 97 (1974); A.C. Scott, F.Y.F. Chu, and D.W. McLaughlin, Proc. IEEE 61, 1443 (1973).

14. G.M. Gasymov and B.M. Levitan, Russian Math. Surveys 19, 1 (1964); V. Barcilon, J. Math. Phys. 15, 429 (1974); B.N. Zachariev, B.V. Rudyak, A.A. Suzko, and I.B. Ushakov, JINR, Dubna report No. P4-8640 (1975, unpublished).

15. Thacker, Quigg, and Rosner, first paper of ref. 7.

16. Schonfeld, et al., ref. 7.

17. With $\rho=1$, this relation (up to the color factor) is due to R. Van Royen and V.F. Weisskopf, Nuovo Cim. 50, 617 (1967); ibid., 51, 583 (1967). Multiplicative corrections have been investigated by many authors, including R. Barbieri, et al., Phys. Lett. 57B, 455 (1975), Nucl Phys. B105, 125 (1976); W. Celmaster, Phys. Rev. D19, 1517 (1979); E. Poggio and H.J. Schnitzer, ibid., D20, 1175 (1979);

ibid., D21, 2034 (1980); L. Bergström, H. Snellmann, and G. Tengstrand, Phys. Lett. 80B, 242 (1979); ibid., 82B, 419 (1979); Z. Phys. C4, 215 (1980); C. Michael and F.P. Payne, Phys. Lett. 91B, 441 (1980); B. Durand and L. Durand, Wisconsin preprint No. DOE/ER/00881-176 (1980, unpublished).

18. Particle Data Group, Rev. Mod. Phys. 52, S1 (1980).

19. Thacker, Quigg, and Rosner, second paper of ref. 7.

20. We use the spectroscopic notation $n^{(2S+1)}L_J$, where n is the principal quantum number, related to the radial quantum number n_r by $n=n_r+\ell$.

21. P. Moxhay, J.L. Rosner, and C. Quigg, Fermilab-Pub-81/14-THY, following paper.

22. See the discussion in Quigg, ref. 1. Fine structure depends upon the Lorentz structure of the potential, as well as its shape. E. Eichten and F. Feinberg, Phys. Rev. Lett. 43, 1205 (1979) and Harvard preprint 80/A053 (unpublished) have achieved a partial understanding of spin-dependent forces in QCD.

23. E. Eichten, et al., Phys. Rev. D17, 3090 (1978).

24. L.M. Lederman, in Proceedings of the 19th International Conference on High Energy Physics, Tokyo, 1978, edited by S. Homma, M. Kawaguchi, and H. Miyazawa (Physical Society of Japan, Tokyo, 1979), p. 706.

25. We thank S. Herb for a discussion of this possibility.

26. See, for example, E. Eichten and K. Gottfried, Phys. Lett. 66B, 286 (1977).

27. C. Quigg and J.L. Rosner, Phys. Lett. 72B, 462 (1978).

28. If the 4^3P_1 level lies in the approximately 50 MeV/c^2 interval between $2M_B$ and $M_B + M_B^*$ (where B and B* denote the pseudoscalar and vector b-flavored mesons), it may decay appreciably into $T(3S)+\gamma$. In that event, the lower bound of eq. (24) would be weakened to $M_B > 5.2$ GeV/c^2.

29. Measurements have been made by several PETRA experiments. See Ch. Berger, et al. (PLUTO Collaboration), Phys. Lett. 81B, 410 (1979); ibid., 86B, 413 (1979); ibid., 91B, 148 (1980); R. Brandelik, et al. (TASSO Collaboration), ibid., 83B, 261 (1979); ibid., 88B, 199 (1979); ibid., 89B, 418 (1980); Z. Phys. C4, 87 (1980); W. Bartel, et al. (JADE Collaboration), Phys. Lett. 88B, 171 (1979); ibid., 89B, 136 (1979); ibid., 91B, 152 (1980); D.P. Barber, et al., (Mark-J Collaboration), Phys. Rev. Lett. 44, 1722 (1980).

Table I. Quarkonium observables[a] used in constructing potentials.

Level	Mass (GeV/c^2)	Γ_{ee} (keV)
$\psi(1S)$	3.097	4.8
$\psi(2S)$	3.686	2.1
$[\chi_c(2P)]$	3.521	---
$T(1S)$	9.434	1.0
$T(2S)$	9.994	0.45
$T(3S)$	10.324	0.32
$T(4S)$	10.545	0.25

a) The values chosen are taken from Refs. 2,9, and 18.

Table II. Potentials constructed from charmonium.

	Quantity	ρ=1	ρ=1.4	ρ=2
input parameters	E_0 (GeV)	3.8	3.8	3.8
	m_c (GeV/c^2)	1.1	1.4	1.7
	κ_1 (GeV/c)	1.3636	1.5246	1.7199
	κ_2	0.8794	0.9921	1.0932
	κ_3	0.6659	0.7496	0.8305
	κ_4	0.3541	0.3995	0.4402
consequences: ψ	$\langle M(\chi_c)\rangle$ (GeV/c^2)	3.517	3.516	3.519
	$(M(\psi')-\langle M(\chi_c)\rangle)/(M(\psi')-M(\psi))$	0.287	0.289	0.284
	1S: $\langle r\rangle, \langle r^2\rangle^{1/2}$ (GeV^{-1})	2.2,2.5	2.0,2.2	1.8,2.0
	2S: $\langle r\rangle, \langle r^2\rangle^{1/2}$ (GeV^{-1})	5.0,5.5	4.4,4.9	4.0,4.5
consequences: Υ	m_b (GeV/c^2)[a]	4.541	4.797	5.080
	1S: Γ_{ee} (keV)[b]	1.16	0.87	0.77
	$\langle r\rangle, \langle r^2\rangle^{1/2}$ (GeV^{-1})	1.0,1.1	1.0,1.1	0.95,1.1
	2S: M (GeV/c^2)	10.021	9.992	9.999
	$\Gamma(2S)/\Gamma(1S)$	0.28	0.32	0.31
	$\langle r\rangle, \langle r^2\rangle^{1/2}$ (GeV^{-1})	2.6,2.8	2.5,2.7	2.4,2.5
	3S: M (GeV/c^2)	10.361	10.353	10.375
	$\Gamma(3S)/\Gamma(1S)$	0.28	0.28	0.25
	$\langle r\rangle, \langle r^2\rangle^{1/2}$ (GeV^{-1})	3.5,3.9	3.5,3.8	3.4,3.7
	4S: M (GeV/c^2)	10.61	10.57	---
	$\Gamma(4S)/\Gamma(1S)$	0.15	0.10	---
	$\langle r\rangle, \langle r^2\rangle^{1/2}$ (GeV^{-1})	5.5,5.9	6.4,6.8	---
	$(M(T')-M(T))$ (GeV/c^2)	0.587	0.559	0.564
	$(M(T')-\langle M(\chi_b)\rangle)/(M(T')-M(T))$	0.174	0.179	0.158

a) Chosen to give $M(T)=9.434$ GeV/c^2.

b) Assuming that the parameter ρ has the same value for $(c\bar{c})$ and $(b\bar{b})$ systems.

Table III. Potentials constructed from upsilons.

	Quantity	ρ=1	ρ=1.4	ρ=2
input parameters	E_0 (GeV)	10.6	10.6	10.6
	m_b (GeV/c^2)	4.5	4.75	5.0
	κ_1 (GeV/c)	3.0513	3.4108	3.8823
	κ_2	2.2916	2.3544	2.4155
	κ_3	1.9628	2.0455	2.1210
	κ_4	1.6514	1.6966	1.7410
	κ_5	1.4120	1.4659	1.5173
	κ_6	1.1140	1.1446	1.1743
	κ_7	0.8706	0.9033	0.9343
	κ_8	0.4970	0.5107	0.5239
consequences: Υ	$\langle M(\chi_b)\rangle$ (GeV/c^2)	9.852	9.862	9.873
	$(M(\Upsilon')-\langle M(\chi_b)\rangle)/(M(\Upsilon')-M(\Upsilon))$	0.254	0.236	0.216
	1S $\langle r\rangle,\langle r^2\rangle^{1/2}$ (GeV^{-1})	1.1,1.2	1.1,1.2	1.0,1.1
	2S: $\langle r\rangle,\langle r^2\rangle^{1/2}$ (GeV^{-1})	2.5,2.7	2.4,2.6	2.3,2.5
	3S: $\langle r\rangle,\langle r^2\rangle^{1/2}$ (GeV^{-1})	3.8,4.2	3.7,4.0	3.6,3.9
	4S: $\langle r\rangle,\langle r^2\rangle^{1/2}$ (GeV^{-1})	5.3,5.8	5.1,5.6	4.9,5.4
consequences: ψ	m_c (GeV/c^2)[a]	1.082	1.359	1.626
	1S: Γ_{ee} (keV)[b]	4.5	4.8	4.7
	$\langle r\rangle,\langle r^2\rangle^{1/2}$ (GeV^{-1})	2.2,2.5	2.0,2.2	1.8,2.1
	2S: M (GeV/c^2)	3.678	3.676	3.672
	Γ_{ee} (keV)[b]	1.6	1.8	1.8
	$\langle r\rangle,\langle r^2\rangle^{1/2}$ (GeV^{-1})	5.4,5.9	4.6,5.0	4.1,4.5
	$(M(\psi')-M(\psi))$ (GeV/c^2)	0.581	0.579	0.575
	$\langle M(\chi_c)\rangle$ (GeV/c^2)	3.521	3.523	3.516
	$(M(\psi')-\langle M(\chi_c)\rangle)/(M(\psi')-M(\psi))$	0.270	0.264	0.271

a) Chosen to give $M(\psi)=3.097$ GeV/c^2.

b) Assuming that the parameter ρ has the same value for $(c\bar{c})$

Table IV. Masses (in GeV/c^2) of upsilon states in potential models.

Level	Inverse scattering			Ref. 11
	ρ=1	ρ=1.4	ρ=2	
1S	input: 9.434			9.434
2S	input: 9.994			9.994
3S	input: 10.324			10.324
4S	input: 10.545			10.594
2P	9.852	9.862	9.873	9.864
3P	10.211	10.219	10.228	10.224
4P	10.462	10.469	10.476	10.504
3D	10.113	10.120	10.128	10.114
4D	10.393	10.400	10.406	10.404
4F	10.307	10.314	10.320	

Table V. Electric dipole matrix elements and transition rates in charmonium.

Potential	$\langle 1S\|r\|2P\rangle$ (GeV^{-1})	$\Gamma(\chi_J \to \psi+\gamma)$ (keV)	$\langle 2P\|r\|2S\rangle$ (GeV^{-1})	$\Gamma(\psi' \to \chi_J+\gamma)$ (keV)
ψ potentials:				
		(J=2) 674		(J=2) 52
ρ=1	2.47	(1) 505	-3.06	(1) 71
		(0) 242		(0) 80
		(2) 531		(2) 41
ρ=1.4	2.19	(1) 398	-2.71	(1) 56
		(0) 190		(0) 63
		(2) 422		(2) 34
ρ=2	1.95	(1) 316	-2.47	(1) 46
		(0) 151		(0) 52
T potentials:				
		(2) 663		(2) 57
ρ=1	2.45	(1) 497	-3.21	(1) 78
		(0) 238		(0) 88
		(2) 533		(2) 45
ρ=1.4	2.20	(1) 400	-2.86	(1) 62
		(0) 191		(0) 70
		(2) 482		(2) 37
ρ=2	2.09	(1) 361	-2.59	(1) 51
		(0) 173		(0) 57

Table VI. Electric dipole matrix elements and transition rates in the upsilon family.

Potential	$\langle 1S\|r\|2P\rangle$ (GeV^{-1})	$\Gamma(\chi_b \to \Upsilon+\gamma)$ (keV)	$\langle 2P\|r\|2S\rangle$ (GeV^{-1})	$\Gamma(\Upsilon' \to \chi_b+\gamma)/(2J+1)$ (keV)
ψ potentials:				
$\rho=1$	1.07	44	-1.78	0.39
$\rho=1.4$	1.07	37	-1.76	0.36
$\rho=2$	1.00	36	-1.74	0.26
Υ potential:				
$\rho=1$	1.19	35	-1.63	0.87
$\rho=1.4$	1.15	35	-1.63	0.70
$\rho=2$	1.10	34	-1.62	0.53

Table VII. Predicted rates for electric dipole transitions among spin-triplet (bb) states, in two T-potentials.

	ρ=1			ρ=2		
Transition	k_γ (MeV)	$\langle f\|r\|i\rangle$ (GeV^{-1})	$\Gamma/(2J_f+1)$ (keV)	k_γ (MeV)	$\langle f\|r\|i\rangle$ (GeV^{-1})	$\Gamma/(2J_f+1)$ (keV)
2P→1S	409	1.19	11.6	428	1.10	11.3
2S→2P	140	-1.63	0.87	119	-1.62	0.53
3P→2S	216	2.12	5.4	232	1.88	5.3
→1S	747	0.24	2.8	761	0.25	3.2
3S→3P	112	-2.65	1.17	95	-2.65	0.72
→2P	460	-0.042	0.02	440	0.018	0.003
4P→3S	139	3.12	3.1	152	2.73	3.1
→2S	460	0.29	1.0	471	0.32	1.3
→1S	978	0.115	1.48	989	0.110	1.41
4S→4P	83	-3.80	1.00	69	-3.78	0.57
→3P	330	-0.147	0.09	313	-0.038	0.005
→2P	671	0.025	0.02	651	0.015	0.007

FIGURE CAPTIONS

Fig. 1: Potentials constructed from charmonium data collected in Table I, using the parameters given in Table II. (a) $\rho=1$, $m_c=1.1$ GeV/c^2; (b) $\rho=1.4$, $m_c=1.4$ GeV/c^2; (c) $\rho=2$, $m_c=1.7$ GeV/c^2. Levels of the charmonium (upsilon) system are plotted on the left (right). Solid lines denote the $^3S_1$ states; dashed lines indicate the mean mass of the 2^3P_J states. The right-hand scale (for the upsilons) is shifted by an amount $2(m_b-m_c)$ with respect to the left-hand (psion) scale.

Fig. 2: Comparison of the charmonium potentials of Fig. 1 and Table II. Dot-dashed line: $\rho=1$, $m_c=1.1$ GeV/c^2; solid line: $\rho=1.4$, $m_c=1.4$ GeV/c^2; long-dashed line: $\rho=2$, $m_c=1.7$ GeV/c^2. The short-dashed line is the "asymptotic freedom" potential of Buchmüller and Tye, ref. 11, with the scale parameter chosen as $\Lambda_{\overline{MS}}=509$ MeV.

Fig. 3: Comparison of two potentials constructed from the upsilon data in Table I, with the assumption that $\rho=1$. The solid line is for a b-quark mass of 4.5 GeV/c^2; the dashed line corresponds to $m_b=5$ GeV/c^2.

Fig. 4: Potentials constructed from the upsilon data given in Table I, using the parameters listed in Table III. (a) $\rho=1$, $m_b=4.5$ GeV/c^2; (b) $\rho=1.4$, $m_b=4.75$ GeV/c^2; (c) $\rho=2$, $m_b=5$ GeV/c^2. Levels of the upsilon

(charmonium) system are plotted on the right (left). Solid lines denote the $^3S_1$ states; dashed lines indicate the mean mass of the 2^3P_J states. The left-hand scale (for the psions) is shifted by an amount $2(m_c-m_b)$ with respect to the right-hand (upsilon) scale.

Fig. 5: Comparison of the upsilon potentials of Fig. 4 and Table III. Dot-dashed line: $\rho=1.4$, $m_b=4.5$ GeV/c^2; solid line: $\rho=1.4$, $m=4.75$ GeV/c^2; long-dashed line: $\rho=2$, $m_b=5$ GeV/c^2. The short-dashed line is the "asymptotic freedom" potential of Buchmüller and Tye, ref. 11, with the scale parameter chosen as $\Lambda_{\overline{MS}}=509$ MeV.

Fig. 6: Comparison of potentials deduced from the ψ and T families. The energy scale is appropriate for the ψ spectrum. In each graph, the label on the left-hand ordinate refers to the potential constructed using upsilon data (solid curve). The label on the right-hand ordinate refers to the potential constructed using psion data (dashed curve). (a) $\rho=1$; (b) $\rho=1.4$; (c) $\rho=2$.

Fig. 7: Upsilon level schemes in four potentials. Arrows indicate the positions of the observed $^3S_1$ levels. The consequences of the potentials of Table III, constructed from the $^3S_1$ levels of the T system according to inverse scattering methods, are plotted as the dot-dashed lines: $\rho=1$, $m_b=4.5$

GeV/c^2; solid lines: ρ=1.4, m_b=4.75 GeV/c^2; dashed lines: ρ=2, m_b=5 GeV/c^2. Shown for comparison are the predictions (dotted lines) of the Buchmüller-Tye potential of ref. 11.

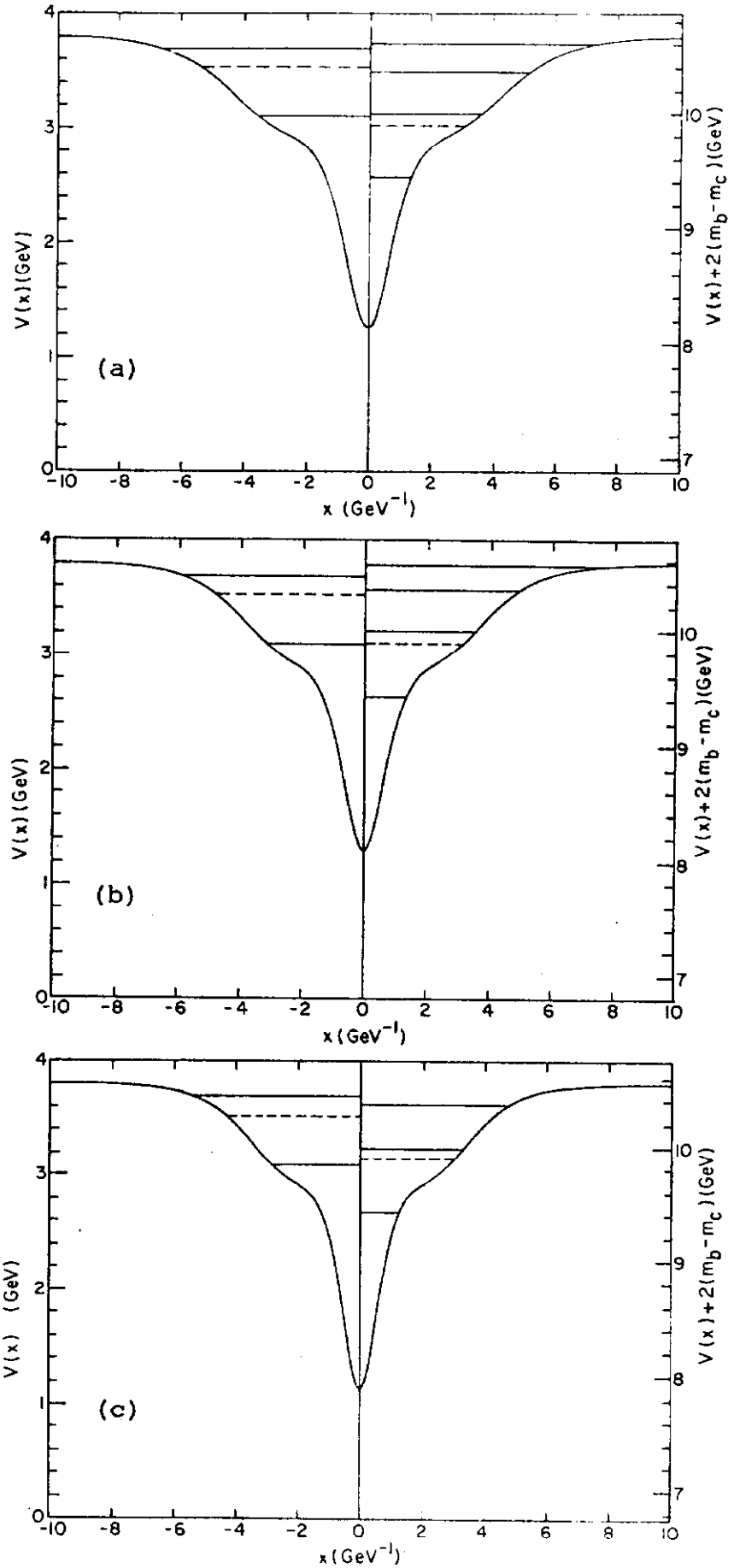

Fig. 1

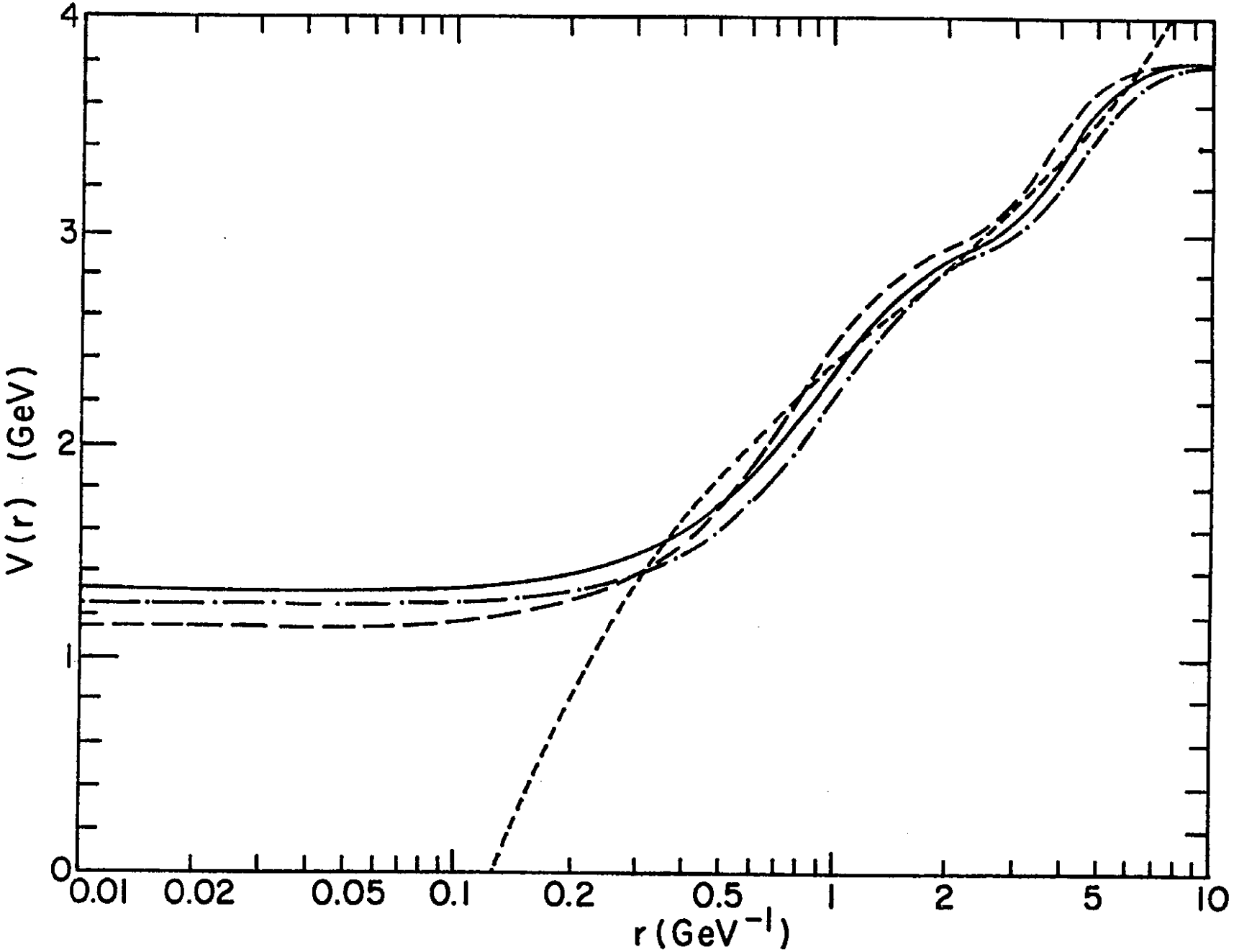

Fig. 2

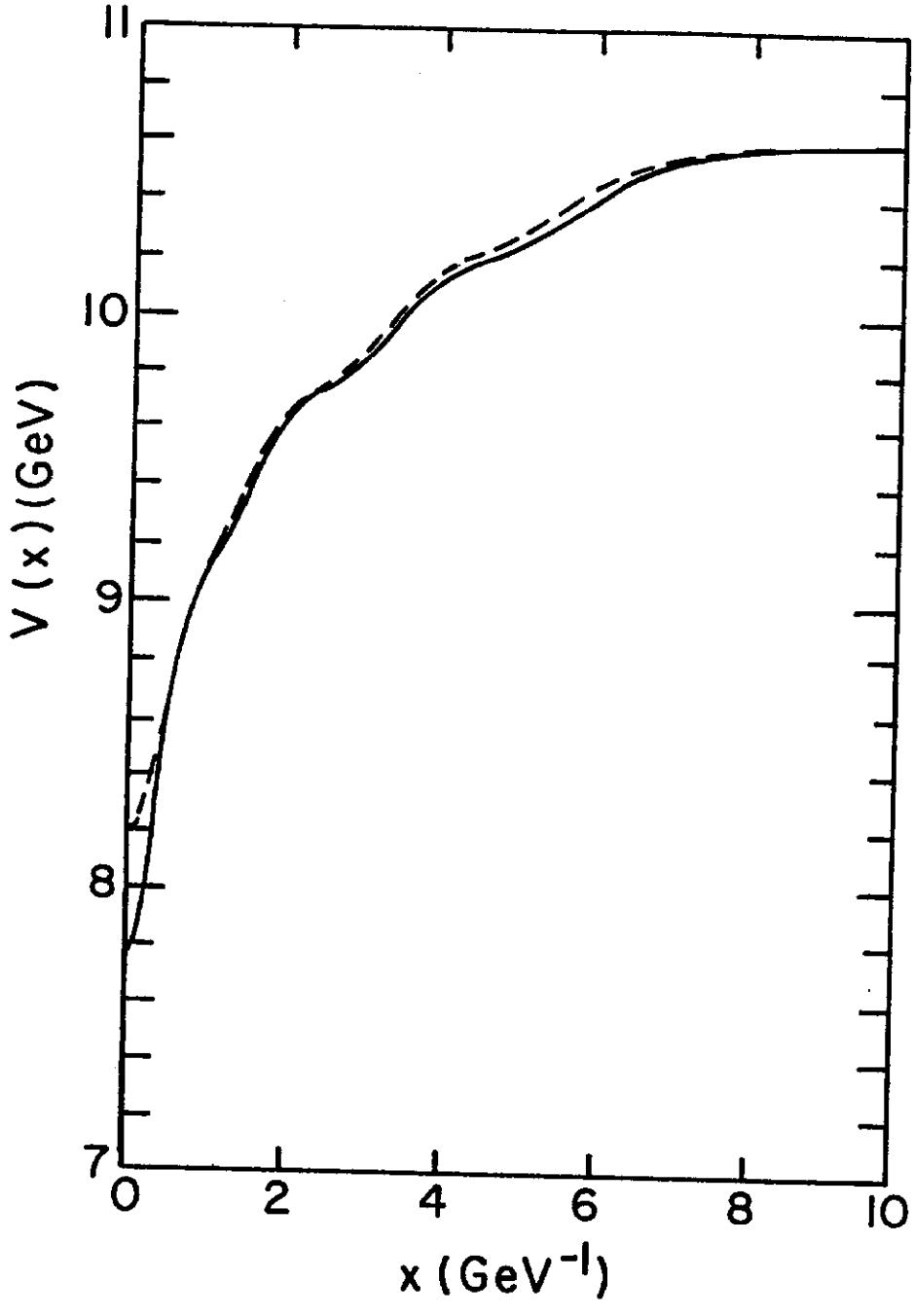

Fig. 3

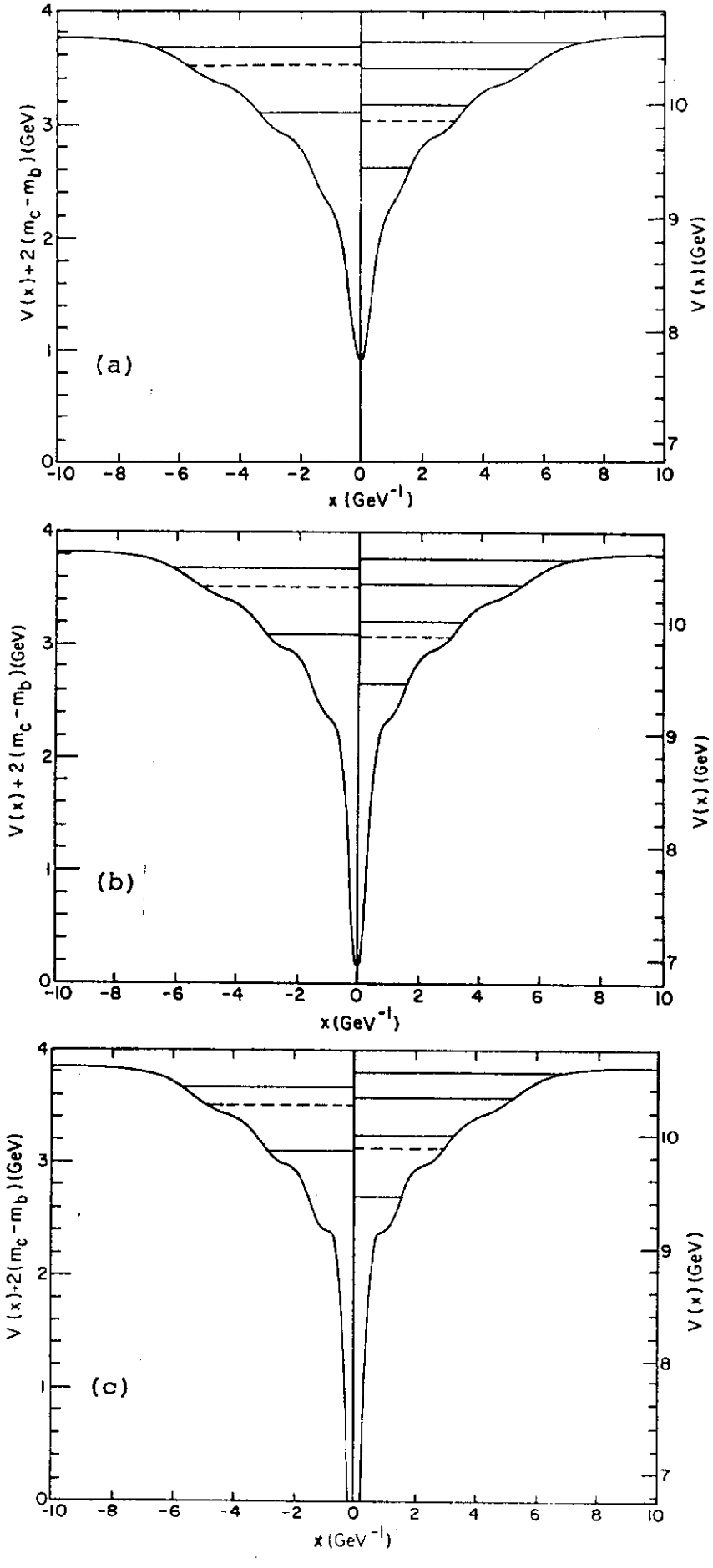

Fig. 4

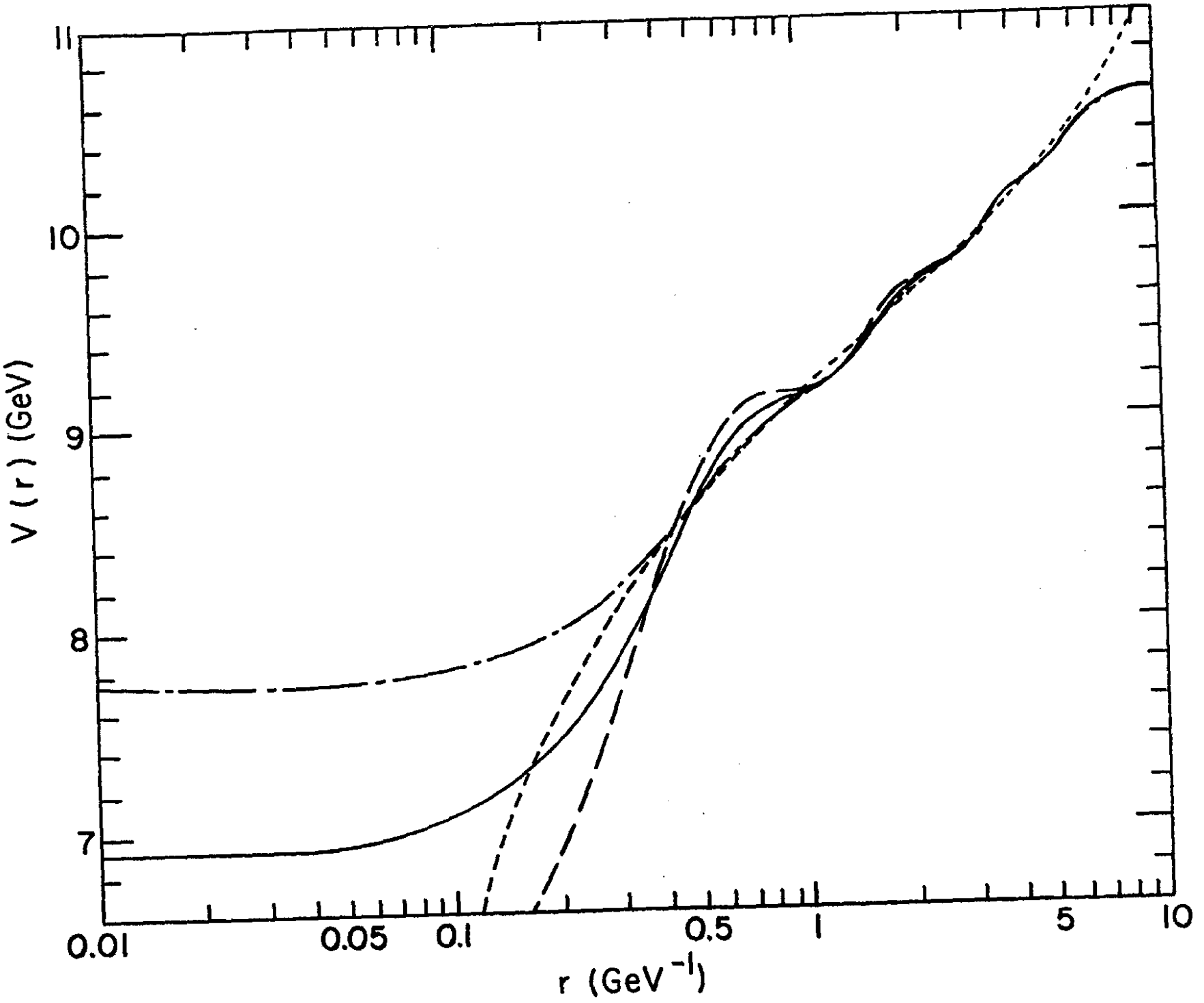

Fig. 5

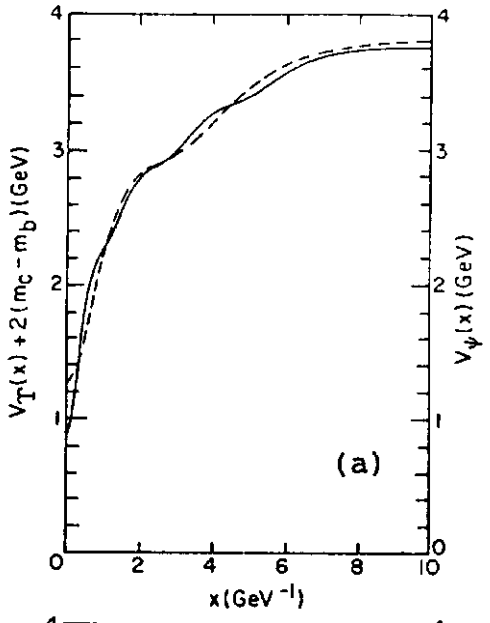
$V_\Upsilon(x)+2(m_c-m_b)$(GeV)
$V_\psi(x)$(GeV)
x(GeV^{-1})
(a)

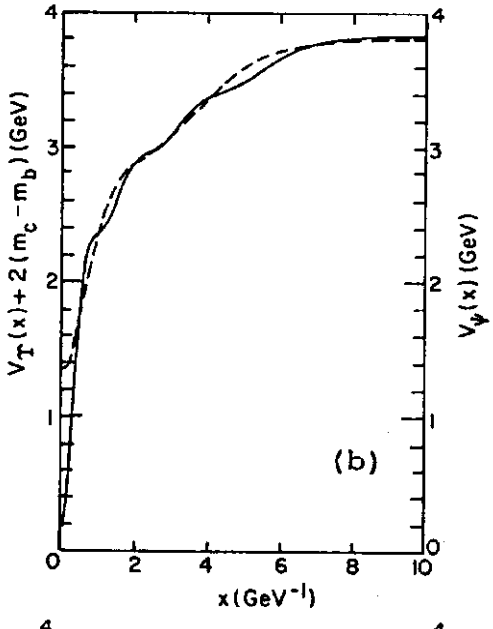
$V_\Upsilon(x)+2(m_c-m_b)$(GeV)
$V_\psi(x)$(GeV)
x(GeV^{-1})
(b)

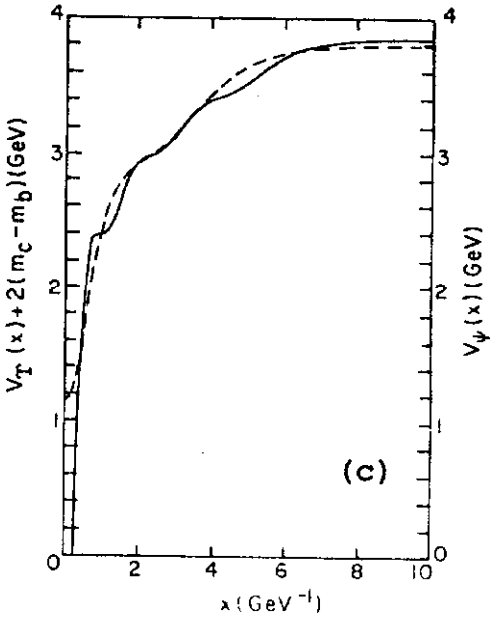
$V_\Upsilon(x)+2(m_c-m_b)$(GeV)
$V_\psi(x)$(GeV)
x(GeV^{-1})
(c)

Fig. 6

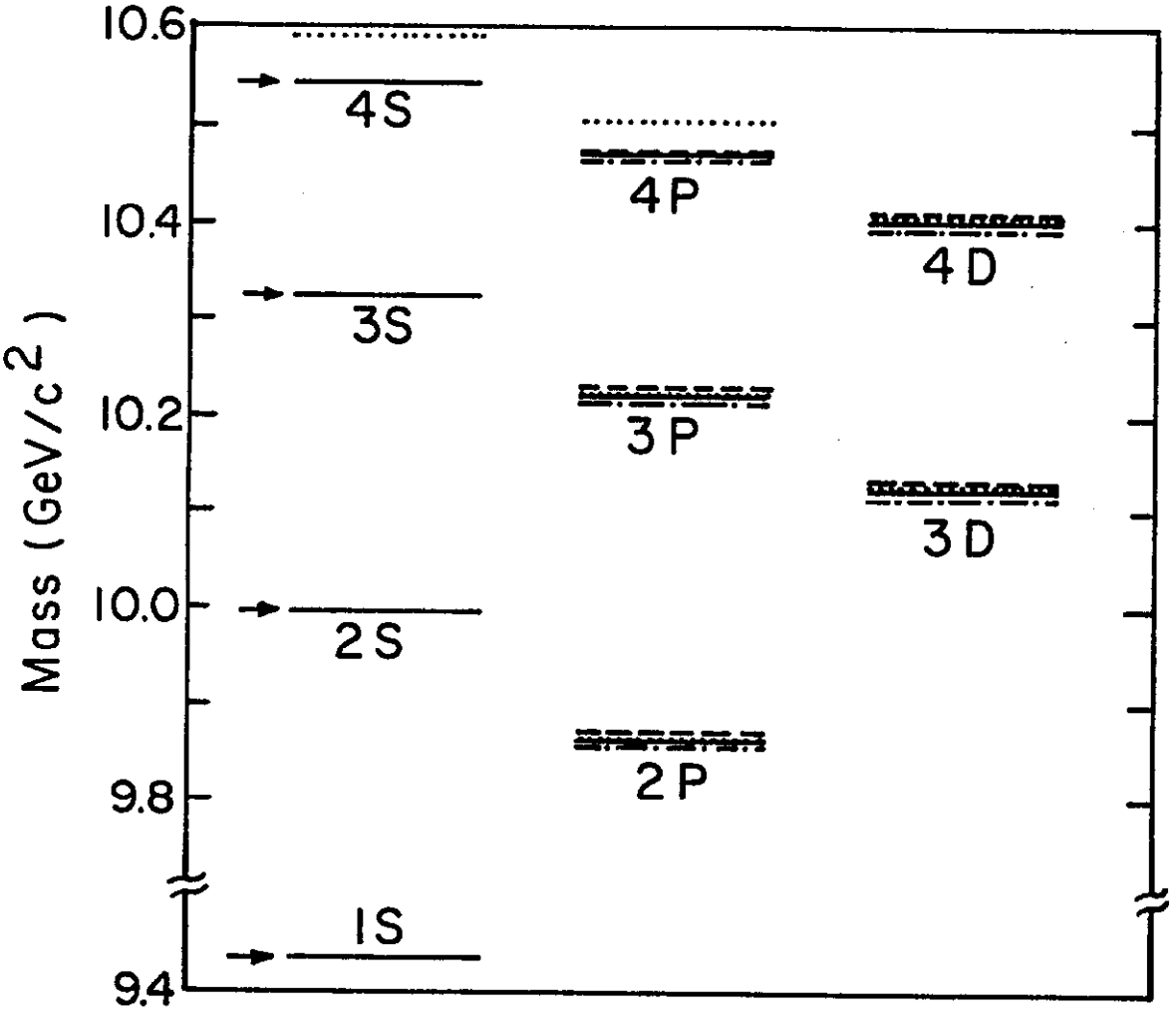

Fig. 7